Journal of Optoelectronic and Biomedical Materials Vol. 15, No. 4, October-December 2023, p. 115-125

Congo red pigment weeding out from water media via RuO_2@ZnO nanostructure

H. Idriss[a,b,*], A. I. Alakhras[b,c], A. Modwi[d]
[a]*Physics Department, College of Science, Imam Mohammad Ibn Saud Islamic University (IMSIU), Riyadh 13318, Saudi Arabia*
[b]*Deanship of Scientific Research, Imam Mohammad Ibn Saud Islamic University (IMSIU), P.O. Box 5701, Riyadh 11432, Saudi Arabia*
[c]*Chemistry Department, College of Science, Imam Mohammad Ibn Saud Islamic University (IMSIU), Riyadh 13318, Saudi Arabia*
[d]*Department of Chemistry, College of Science and Arts, Qassim University, Al-Rass 51921, Saudi Arabia*

In this report, RuO_2@ZnO nanostructure was synthesized, characterized, and employed for Congo Red (CR) dye removal from the aquatic phase. The influence of sorption factors contact time, pH, and concentration, was examined. The results indicates the formation of RuO_2@ZnO nanostructure with surface area of 21 m^2 g^{-1} and pore size of 23.5 nm. . The highest amount of Congo red adsorbed by RuO_2@ZnO nanostructure was 102.42 mg/g. Excellent obedience was found between the equilibrium data and the Langmuir model (R^2 > 0.9338), whereas the adsorption kinetics was consistent with the pseudo-second-order equation (R^2> 0.9999).

(Received August 1, 2023; Accepted October 19, 2023)

Keywords: Congo red, RuO_2@ZnO, Nanostructure, Adsorption, Adsorption kinetics

1. Introduction

Water environmental issues are linked to adverse human effects on the environment. Environmental conservation is a practice that aims to protect the natural environment at the individual, organizational, or governmental level for the benefit of both the environment and people; concepts and laws that work to protect the environment can be developed through awareness, education, and scientific research. Dye pollution is one of the most pressing issues facing the industry. In fact, much of the synthetic dye does not stick, is lost in wastewater associated with manufacturing, and is usually discarded without treatment[1, 2]. Organic dyes are one of the leading factors of pollutants in the water, which is generated by the wastewater discharges of several manufacturing sectors including textiles, plastics, dyeing, photography, printing, and tanning[3]. Congo red is a principal family of synthetic colorants azo dyes are commonly employed in textile production owing to their characteristics, which include a wide range of hues, resistance to decolorization, and low energy requirements[4]. It is known that Congo red is cancer causing due to its aromatic amine content[5]. Since Azo dyes contain aromatic structures, they are resistant to natural breakdown[6].

Dye pollution harms the environment because it lingers in the environment for a very long time. Congo red pigment prevents the water from reoxygenating properly due to its presence[7]. Upon ingesting, this contaminant causes irritation of the eyes and skin, stomach discomfort, nausea, vomiting, and diarrhea[8]. Therefore, Congo Red dyes tainted water needs to be treated[9].The wastewater treatment methods can be accomplished in a broad range of methods, for instance electrocoagulation, filtration, chemical precipitation, flotation, ozonation, membrane processes, electrocoagulation and adsorption[10, 11]. Adsorption is considered to be the most practical strategy of all those documented techniques so far[12]. This is due to its high efficiency, simplicity,

* Corresponding author: hiidriss@imamu.edu.sa
https://doi.org/10.15251/JOBM.2023.154.115

and minimal energy consumption[13]. A suitable model for removing Congo red has been developed using the adsorption process[14, 15]. This led to the investigation of various adsorbents with different adsorption capacities[16].

Currently. It has been demonstrated that the application of nanotechnology in the remediation of polluted environments is helpful, as it not only takes less time but also brings the level of pollutants down to the minimum allowable values[17]. Nanostructured materials have been used utilized in multiple ecological sectors, including treating contaminated water, cultivation, and much more cutting-edge uses than conventional techniques[18]. According to nanoscience, many of the current problems with water pollution can be solved or prevented through the use of nanotubes, nanofilms, nanodiscs, and nanosensors[19].Nanotechnology investigation has quickly advanced, offering new approaches to environmental cleanup[20]. Scientists recently put a great deal of emphasis on metallic nanoparticles and heterostructured nanopowder of appropriate shape and size because of their superior properties and capabilities in absorbing dyes effluent[21]. In recent studies, it was shown that metallic oxides with high activity and surface area are highly effective sorbents for the treatment of waste water[22].The design of nanoscale subistances have been manifctured by means of differants physical,chemical ,mechnical and biological routes [23, 24].Several nanoparticles and nanocomposites such as MgO ,TiO_2 ,ZnO , TiO/V_2O_5 , MgO/Se and MgO@ g-C_3N_4 were employed to eliminate Cango red dye and other organic dyes from aqueous media[25-30].

2. Methodology

2.1. Fabrication of RuO2@ZnO nanostructure

In a 1000 mL beaker 0.003 M (Zn $(NO3)_2.2H_2O$), 0.64g of RuCl3 were mixed with the appropriate quantity of pectinose solution with constant heating and agitation at 392°F for 4 hours. Bleached brown foam was produced and kept at room temperature for 20 hours. The bleached brown foam powder was dried and annealed for 2 hours at 248°F. Further, the prepared RuO2-ZnO nanostructure was examined for their structural, morphological, and chemical bonding using different techniques and then employed for CR dye removers.

2.2. Adsorption equilibrium

A 500 ppm standard solution of Congo red (CR)pigment was achieved with distilled water. Afterward, 10 ml of (CR) with concentrations of 10 up to 140 ppm were introduced to 0.0066 g of Ru@ZnO nanomixture. The mixture was shaked under orpital shaker (250 rpm) for 140 minutes. The mixture was filtered after performing an equilibrium purification experiment, and the remaining concentration of CR was measured by a UV spectrophotometer (λ_{max} 620 nm).)[28].

3. Results and discussion

3.1. Ru@ZnO nanostructure characterization

3.1.1. XRD profile of RuO_2@ZnO

X-ray diffractometer (XRD) was implemented to identify the crystallographic nature of the fabricated RuO2@ZnO adsorbent.

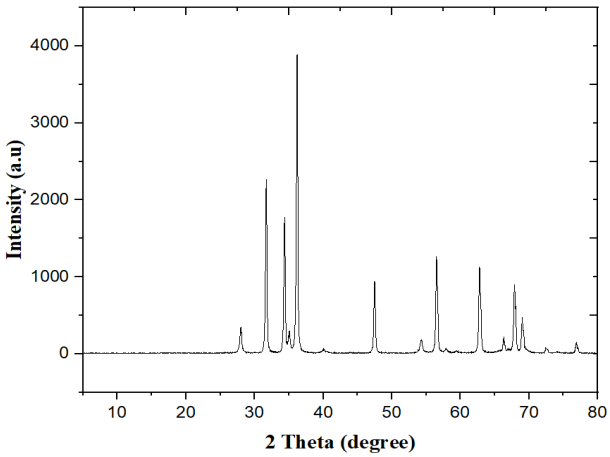

Fig. 1. XRD patents of RuO_2@ZnO nanostructure.

From the figure, it can be recorded that various sharp peaks were observed at two theta = 31.6, 34.4, 36.2, 47.4, 56.5, 62.7, 66.3, 69.0, and 69.3 are assigned to (100), (002), (101), (102), (110), (103), (200), (112), and (201) planes, respectively, of the wurtzite hexagonal ZnO crystalline nature. In compliance with JCPDS card number 88-0322, new peaks matching to 2 theta = 28.0, 35.0, and 54.4 were identified, characterizing the RuO2 rutile phase's (110), (101), and (211) planes[31]. On the basis of XRD patterns, Scherer's approach was utilized to compute the average crystallite size of nanostructurecompound [26].The average crystallite size of the RuO2@ZnO nanostructure compound were found to be to be 39.4 nm.

3.1.2. SEM and EDX analysis of RuO_2@ZnO nanostructure

Field emission scanning electron microscopy (FE-SEM) combined with energy-dispersive X-ray spectrometry was employed to examine the morphological characteristics and the elemental content of RuO2@ZnO nanomixture.

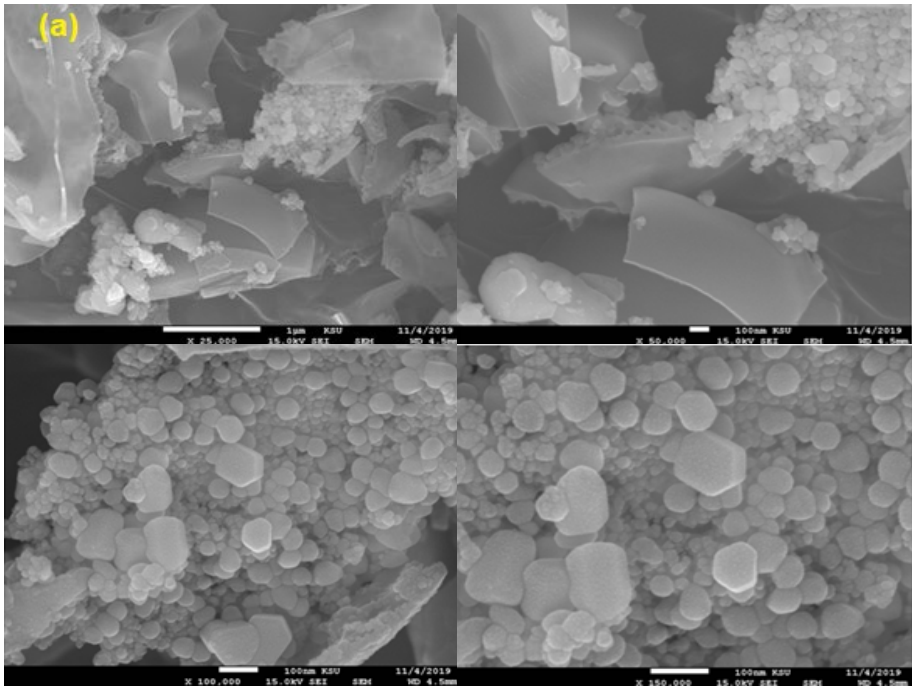

Fig. 2.1. SEM images analysis of RuO_2@ZnO nanostructure (

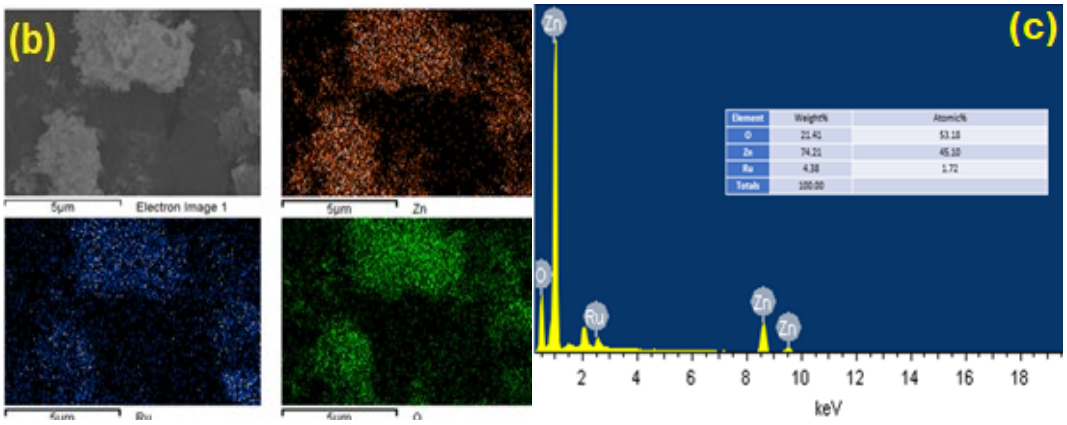

Fig. 2.2) EDX analysis of RuO_2@ZnO nanostructure
b) Elemental mapping(c) Elemental percentage.

As demonstrated in Figure 2, the morphology features of Ru-doped ZnO are distinctly defined and less aggregation and more homogeneity and has rounded shape (fig 2a). Elemental mapping is an accepted approach for confirming the presence of ruthenium in the matrix of zinc oxide nanoparticles forming the RuO2@ZnO nanocomposite; therefore, it was carried out as depicted in figure2b. The EDX profile of the obtained composite (fig 2c) reveals characteristic Ru, Zn, and O peaks, confirming the purity of the synthesized composite.

3.1.3. FTIR analysis of RuO_2@ZnO nanostructure

The chemical bonding and content of the produced RuO2@ZnO nanostructure compound was analyzed by FTIR spectroscopy. Figure (3) displays the FTIR patterns recorded at 500–4000 cm−1 for RuO2@ZnO nanostructure The vast peak at 3378–3395 cm−1 corresponds to the O–H stretching vibration of the acetate -COOH precursor and adsorbed H2O humidity. There is a close correspondence between the wavelength of stretching at 482 cm1 and the Zn–O bonding, which proves that ZnO is formed. Absorption of CO2 in the environment is accountable for the measurable peak at 2346 cm-1, caused by C=O stretching vibrations in the atmosphere[32]. The FTIR profile of Ru@ZnO demonstrates a noticeable peak at 484 cm1, representing the stretching vibrations of Zn-O. Furthermore, FTIR analysis of RuO2@ZnO nanostructure concurred with XRD data.

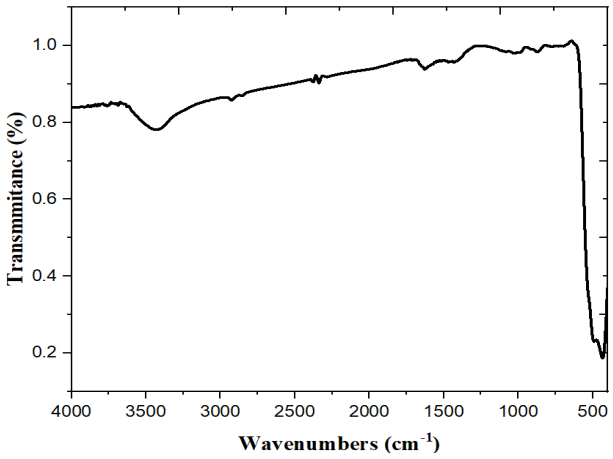

Fig. 3. FTIR spectra of RuO_2@ZnO nanostructure.

3.1.4 Surface area analysis (BET)

The surface area features of RuO2-ZnO nanostructure were analyzed employing Brunauer Emmett Teller(BET) instrument and the Barrett Joyner Halenda (BJH) graph.

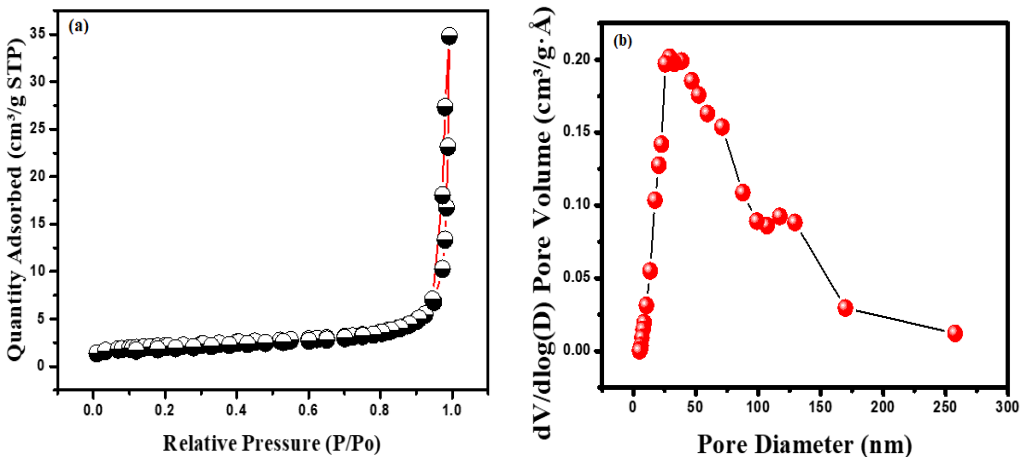

Fig. 4. Adsorption-desorption isotherms of N_2 at 77 K with (inset) Pore size distribution of RuO_2@ZnO nanostructure.

The N2 sorption isotherm results demonstrated that the isotherm is Langmuir type IV (Fig. 4) with relative pressure (P/Po = 0.0-1.0). Furthermore, the hysteresis loop is of type H3 (Fig. 4(inset)), confirming the nanostructured mesoporous nature with slit-shaped pores [33]. The chart result is in the mesoporous range of 0 to 100, corresponding to the type IV adsorption isotherm representation according to the IUPAC classification[34] . RuO2-ZnO has a specific surface area of 21 m2 g-1. Furthermore, the pore size distribution and volume were 23.5 nm and 0.066cm3g-1, respectively.

3.2. Removal of CR dye via RuO_2@ZnO nanostructure

3.2.1. Influence of the Initial CR dye concentration

The role of a starting CR dye concentration in on the sorption performance of a RuO2@ZnO nanostructure was evaluated at concentration from 10 ppm to 140 ppm as demonstrated in figure 5. The removal rate increases whenever the dye concentration is low and decreases with increasing concentration. Noticed that At 10 ppm the removal rate was 96%, 20 ppm (93%) , 40 ppm (80%), 80 ppm (55%), 120 ppm(54%) and 140 ppm (49%). Because of the vast number of unoccupied active sites, CR in the reaction media interacts more efficiently with the top layer of the sorbent[35]. Therefore, decreased available areas for CR are seen when concentration increases due to possible saturation with CR.

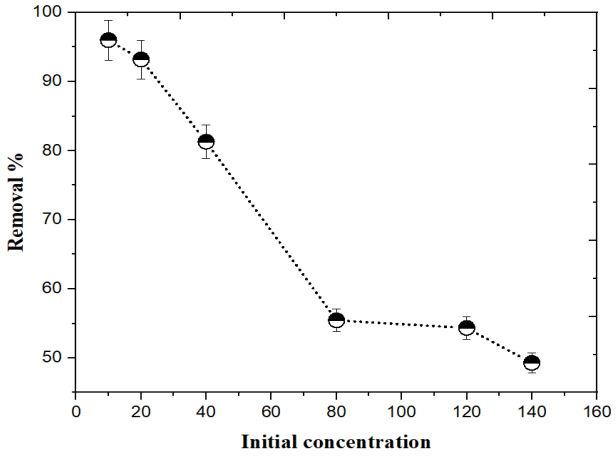

Fig. 5. Influence of the Initial CR dye concentration.

3.2.2. Influence of pH on CR removal

The constructed RuO_2@ZnO nanostructure was used to assess the role of pH on CR dye sorption functionality.

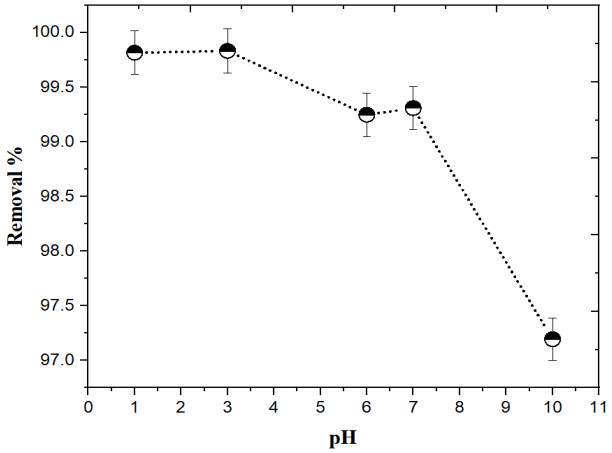

Fig. 6. pH of CR solution against removal percentage.

Accordingly, the pH of the sorption process influences the interaction between the dye molecule and the sorbate[36]. Hence, the uptake capacity of the adsorbent effect of the dye solution's initial pH on the adsorption of RuO_2@ZnO nanostructure on CR was systematically evaluated. As a result, the CR sorption capacities displayed different oscillating patterns owing to their distinct electronegativity[37], as seen in figure(6) . The removal % was risen dramatically At pH 1 to 3 , for from pH 6 to 7 CR sorption % remained constant , on the other hand at pH 10 the removal % decreased as depicted in figure (7). Chemical sorption was found to be the dominant pathway in the sorption of CR onto RuO2@ZnO nanostructure.

3.2.3. Influence of contact time on removal

The adsorption capabilities of RuO_2@ZnO nanostructure against CR dye contact time were examined in figure (7). From the figure, the removal rate of Cr increases with increasing contact time. The equilibrium adsorption capacity occurred at 120 minutes, indicating that RuO2@ZnO nanostructure preferentially absorbs RuO2@ZnO nanostructure in the ambient pH environment. The formation of a dye molecular layer on the surface of the RuO2@ZnO nanostructure likely contributed to the dye molecules' resistance to sorption[38].

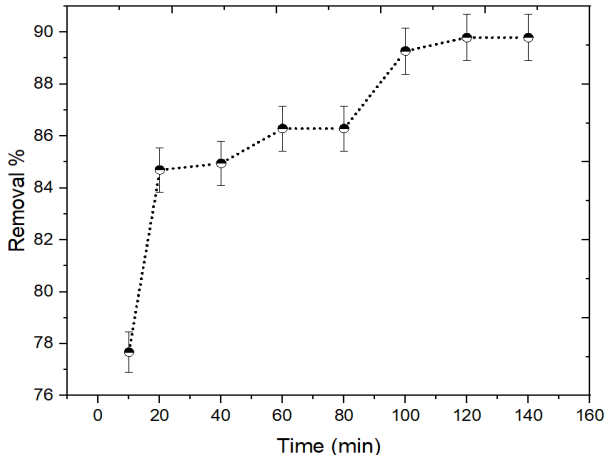

Fig. 7. Contact time against removal percentage.

3.3. Adsorption isotherms and kinetics

The ability of the sorbents to remove CR dye has been evaluated using Freundlich and Langmuir isotherms[39] figure (8).

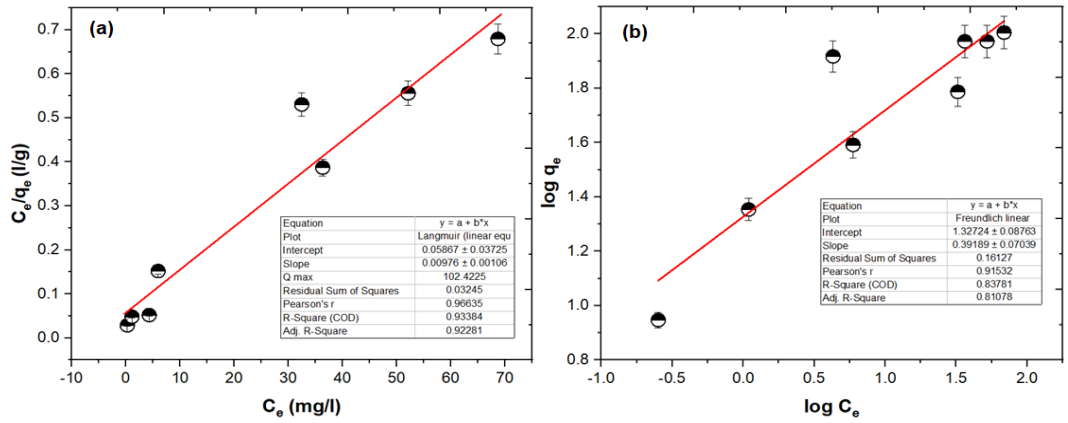

Fig. 8. Plot of isotherm models adsorption (a) linearized Freundlich model (b) linearized Langmuir model.

Table 1 displays the associated computed isotherm parameters for CR dye sorption on Ru@ZnO. To examine the kinetics of the CR dye adsorption process onto Ru@ZnO nanomixture, both the pseudo-first-order model and the pseudo-second-order model were analyzed[40] figure (9). The results of the derived kinetics variables are given in table 2. The kinetic data demonstrated that the adsorption of CR dye follows the pseudo-second-order kinetic model (R2 = 0.9999). Therefore, adsorption is a monolayer coverage process. Moreover, there was a variation between experimental and theoretical qe values. Ru@ZnO nanostructure have outstanding adsorption performance for CR dye, with a maximum adsorption capacity of 102 mgg-1.

Table 1. Adsorption equilibrium constants for the dye removal RuO_2@ZnO nanostructure.

	Langmuir constants				Freundlich constants		
	$q_m(mg.g^{1})$	$K_L(l.mg^{1})$		r^2	n	k_f	r^2
	102.422	0.1664		0.9338	2.552	21.244	0.8378

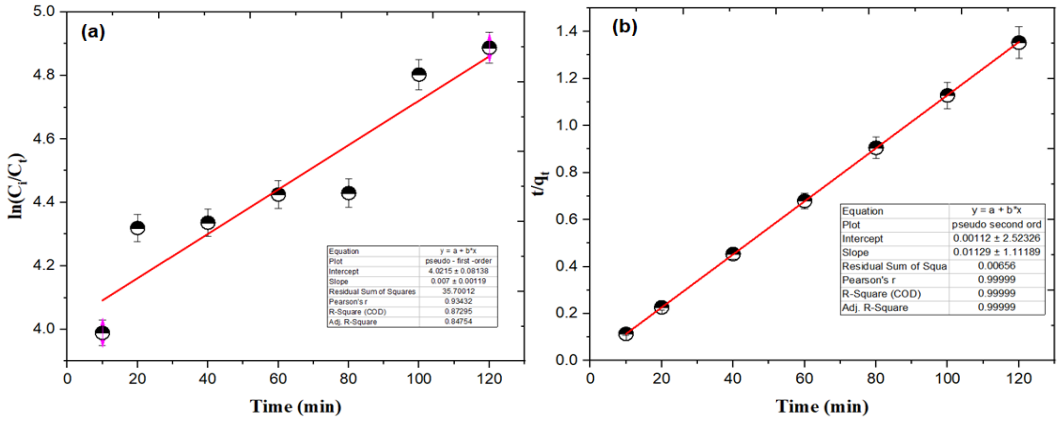

Fig. 9. Kinetics adsorption process (a) pseudo-first-order model (b) pseudo-second-order model.

Table 2. Pseudo-first-order, Pseudo-Second order kinetic parameters for the dye sorptionvia RuO2@ZnO nanostructure.

Kinetic model	parameters	Value
Pseudo-first-order	$q_{m\ (experimental\ )}$ [a]	102
	k_1 (g/mg min)	0.007
	$q_{m(calculated\ )}$ [b]	56.4
	r^2	0.8729
Pseudo-Second order	K_2 (g/mg min)	0.573
	$q_{m(cal)}$ [b]	89.3
	r^2	0.9999

The performance of RuO2@ZnO nanostructure to eliminate the CR dye from aqueous media was compared with other adsorbents mentioned in the published research. As seen in Table 3, the produced RuO2@ZnO nanostructure has a higher capacity for eliminating CR dye than reported sorbents. Therefore RuO2@ZnO nanostructure is considered one of the most promising adsorbents for removing organic pigment from water media.

Table 3. Adsorption capability of different sorbents for CR dye elimination.

Adsorbents	adsorption capacity mg/g	References
Coir pith carbon	6.70	[41]
Fungus Aspergillus	14.72	[42]
Industrial waste	22.12	[8]
cattail root	38.79	[43]
PANI/ZTO nanocomposite	64.51	[44]
Zn(cur)O NPs	70.86	[45]
Chitosan NPs	93.40	[46]
Fe_3O_4@Zn	59.00	[47]
Mycosynthesized FeNPs	48.7	[48]
Fe3O4@CA NPs	46.94	[49]
CuO NPs	35.00	[50]
RuO_2@ZnO	102.42	Current study

4. Conclusion

The produced RuO_2@ZnO nanostructure in the presence of pectinose exhibited high sorption for removing CR pigment from an aqueous solution. Furthermore, the physicochemical profile analysis indicates the formation of RuO_2@ZnO nanostructure with a relatively high surface area of 21 m^2 / g and pore size of 23.5 nm. This shows the construction of RuO_2@ZnO nanostructure with surface area (21 m^2 / g) (20 nm). The highest amount of Congo red adsorbed by RuO_2@ZnO nanostructure was 102.42 mg/g. Excellent obedience was found between the equilibrium data and the Langmuir model (R2 > 0.9338), whereas the adsorption kinetics was consistent with the pseudo-second-order equation (R2 > 0.9999).

Acknowledgements

The authors extend their appreciation to the Deanship of Scientific Research, Imam Mohammad Ibn Saud Islamic University (IMSIU), Saudi Arabia, for funding this research work through Grant No. (221412017).

References

[1] Choudhary, S., et al., ACS Applied Materials & Interfaces, 2023; https://doi.org/10.1021/acsami.2c20710

[2] Rezaeifard, A., et al., ACS Omega, 2023; https://doi.org/10.1021/acsomega.2c05971

[3] Tubić, A., et al., Dyes and Pigments, 2023. 209: p. 110884; https://doi.org/10.1016/j.dyepig.2022.110884

[4] Iark, D., et al., Bioresource technology, 2019. 289: p. 121655; https://doi.org/10.1016/j.biortech.2019.121655

[5] Maruthupandy, M., et al., Journal of Photochemistry and Photobiology A: Chemistry, 2022. 430: p. 113972; https://doi.org/10.1016/j.jphotochem.2022.113972

[6] Mittal, Y., et al., Chemical Engineering Journal, 2022. 427: p. 131856; https://doi.org/10.1016/j.cej.2021.131856

[7] Ikram, M., et al., Zeitschrift für Physikalische Chemie, 2022; https://doi.org/10.1515/zpch-2022-0150

[8] Harja, M., G. Buema, D. Bucur, Scientific Reports, 2022. 12(1): p. 6087; https://doi.org/10.1038/s41598-022-10093-3

[9] Zong, E., et al., International Journal of Biological Macromolecules, 2023. 226: p. 443-453; https://doi.org/10.1016/j.ijbiomac.2022.11.317
[10] Shokri, A. and M.S. Fard, Chemosphere, 2022. 288: p. 132355; https://doi.org/10.1016/j.chemosphere.2021.132355
[11] 11. Alavijeh, H.N., et al., Cleaner Chemical Engineering, 2022. 3: p. 100032; https://doi.org/10.1016/j.clce.2022.100032
[12] Aldaghri, O., et al., Diamond and Related Materials, 2022. 129: p. 109315; https://doi.org/10.1016/j.diamond.2022.109315
[13] Ali, M., et al., Materials Letters, 2022. 322: p. 132501; https://doi.org/10.1016/j.matlet.2022.132501
[14] Jiang, R., et al., Ozone: Science & Engineering, 2020. 42(2): p. 174-182; https://doi.org/10.1080/01919512.2019.1635432
[15] Oladoye, P.O., et al., Groundwater for Sustainable Development, 2022: p. 100844; https://doi.org/10.1016/j.gsd.2022.100844
[16] Ozola-Davidane, R., et al., Journal of Molecular Liquids, 2021. 337: p. 116373; https://doi.org/10.1016/j.molliq.2021.116373
[17] Chowdhury, A., et al., Journal of Environmental Chemical Engineering, 2023. 11(1): p. 109199; https://doi.org/10.1016/j.jece.2022.109199
[18] Liu, J., et al., Journal of environmental management, 2019. 238: p. 473-483; https://doi.org/10.1016/j.jenvman.2019.03.009
[19] Wong, J.K.H., et al., Journal of environmental chemical engineering, 2019. 7(4): p. 103261; https://doi.org/10.1016/j.jece.2019.103261
[20] Baruah, A., et al., Nanotechnology in Water and wastewater treatment. 2019, Elsevier. p. 337-368; https://doi.org/10.1016/B978-0-12-813902-8.00017-4
[21] Okpara, E.C., et al., Environmental Advances, 2023: p. 100341; https://doi.org/10.1016/j.envadv.2023.100341
[22] Kumari, H., et al., Applied Physics A, 2023. 129(2): p. 91; https://doi.org/10.1007/s00339-022-06288-0
[23] Idriss, H., et al., Journal of Optoelectronic and Biomedical Materials Vol, 2022. 14(2): p. 53-61; https://doi.org/10.15251/JOBM.2022.142.53
[24] Idriss, H., et al., Digest J Nano mat Bio struct, 2017. 12: p. 1069-1073.
[25] Idriss, H., Journal of Optoelectronic and Biomedical Materials, 2021. 13(4): p. 183-192; https://doi.org/10.15251/JOBM.2021.134.183
[26] Idriss, H., M. Ibrahem, A. Modwi, Zeitschrift für Naturforschung A, 2023. 78(1): p. 67-76; https://doi.org/10.1515/zna-2022-0166
[27] Modwi, A., et al., Zeitschrift für Naturforschung A, 2018. 73(11): p. 975-983; https://doi.org/10.1515/zna-2018-0219
[28] Idriss, H., A. Alakhras, H. El Khair, Chalcogenide Letters, 2021. 18(10): p. 629-638; https://doi.org/10.15251/CL.2021.1810.629
[29] Modwi, A., et al., Description and Adsorption Mechanism. Inorganics, 2022. 10(11): p. 210; https://doi.org/10.3390/inorganics10110210
[30] Idriss, H. and A. Alakhras, Journal of Optoelectronic and Biomedical Materials, 2020. 12(4): p. 109-119; https://doi.org/10.15251/JOBM.2020.124.109
[31] Abdallah, E.M., et al., Molecules, 2022. 27(23): p. 8309; https://doi.org/10.3390/molecules27238309
[32] Al-Awaji, N., et al., Advances in Materials Science and Engineering, 2022. 2022; https://doi.org/10.1155/2022/9174538
[33] Ramesh, K., et al., Communications in soil science and plant analysis, 2014. 45(16): p. 2171-2181; https://doi.org/10.1080/00103624.2014.929699
[34] Sotomayor, F.J., K.A. Cychosz, M. Thommes, Acc. Mater. Surf. Res, 2018. 3(2): p. 34-50.

[35] Najafi, M., et al., Journal of Industrial and Engineering Chemistry, 2022. 116: p. 489-503; https://doi.org/10.1016/j.jiec.2022.09.039
[36] Ofomaja, A.E., Biochemical Engineering Journal, 2008. 40(1): p. 8-18; https://doi.org/10.1016/j.bej.2007.11.028
[37] Wu, L., et al., Scientific reports, 2021. 11(1): p. 10640; https://doi.org/10.1038/s41598-021-90235-1
[38] Zhang, Q. and G. Cao, Nano today, 2011. 6(1): p. 91-109; https://doi.org/10.1016/j.nantod.2010.12.007
[39] Obaid, S.A. Langmuir, Journal of Physics: Conference Series. 2020. IOP Publishing; https://doi.org/10.1088/1742-6596/1664/1/012011
[40] Moussout, H., et al., Karbala International Journal of Modern Science, 2018. 4(2): p. 244-254; https://doi.org/10.1016/j.kijoms.2018.04.001
[41] Namasivayam, C., D. Kavitha, Dyes and pigments, 2002. 54(1): p. 47-58; https://doi.org/10.1016/S0143-7208(02)00025-6
[42] Fu, Y. and T. Viraraghavan, Advances in Environmental Research, 2002. 7(1): p. 239-247; https://doi.org/10.1016/S1093-0191(01)00123-X
[43] Hu, Z., et al., Journal of Hazardous materials, 2010. 173(1-3): p. 292-297; https://doi.org/10.1016/j.jhazmat.2009.08.082
[44] Singh, S., S. Perween, A. Ranjan, Journal of Environmental Chemical Engineering, 2021. 9(3): p. 105149; https://doi.org/10.1016/j.jece.2021.105149
[45] Arab, C., R. El Kurdi, D. Patra, Materials Today Chemistry, 2022. 23: p. 100701; https://doi.org/10.1016/j.mtchem.2021.100701
[46] Khan, Z., S.A. Al-Thabaiti, International Journal of Biological Macromolecules, 2022. 194: p. 580-593; https://doi.org/10.1016/j.ijbiomac.2021.11.101
[47] Pietrzyk, P. et al., Magnetochemistry, 2022. 8(8): p. 91; https://doi.org/10.3390/magnetochemistry8080091
[48] Singh, G., V. Kumar, S.K. Dwivedi, Journal of Cluster Science, 2022. 33(5): p. 1889-1905; https://doi.org/10.1007/s10876-021-02096-3
[49] Pawar, A.A. et al., Particle & Particle Systems Characterization, 2022: p. 2200156; https://doi.org/10.1002/ppsc.202200156
[50] Khit, S.A., E.T. Kareem, I.M. ShaheedBaghdad Science Journal, 2023l https://doi.org/10.21123/bsj.2023.7444